DALTON

Co-ordinative properties of a hybrid phosphine–bipyridine ligand

Raymond Ziessel,*[,a] Loïc Toupet,[b] Sylvie Chardon-Noblat,[c] Alain Deronzier[c] and Dominique Matt*[,d]

[a] *Laboratoire de Chimie, d'Electronique et de Photonique Moléculaires, Ecole Européenne de Chimie, Polymères, Matériaux (ECPM), Université Louis Pasteur, 1 rue Blaise Pascal, F-67008 Strasbourg Cedex, France*
[b] *Groupe Matière Condensée et Matériaux, Université de Rennes 1, Bât. 11B, Campus Beaulieu, F-35042 Rennes Cedex, France*
[c] *Laboratoire d'Electrochimie Organique et de Photochimie Rédox, Université Joseph Fourier Grenoble 1, BP 53, F-38041 Grenoble Cedex 9, France*
[d] *Groupe de Chimie Inorganique Moléculaire, Université Louis Pasteur, 1 rue Blaise Pascal, F-67008 Strasbourg Cedex, France*

6-(2-Diphenylphosphinoethyl)-2,2′-bipyridine, L, has been prepared in three steps from 6-methyl-2,2′-bipyridine: (*i*) metallation followed by reaction with paraformaldehyde; (*ii*) bromination with HBr–$MeCO_2H$; (*iii*) phosphination using $Li(PPh_2)$. Reaction of L with $[\{RuCl_2(CO)_2\}_n]$ in NEt_3–MeOH gave a mixture of *trans*-Cl_2-$[RuCl_2L(CO)]$ **1** and *cis*-Cl_2-$[RuCl_2L(CO)]$ **2**, the L ligand displaying in both complexes a meridional tridentate binding mode. This behaviour was confirmed, in the case of **1**, by an X-ray structural study. Electrochemical oxidation of **1** and **2** is reversible and occurs at $E_{\frac{1}{2}} = 0.80$ V and 1.04 V *vs*. $Ag–Ag^+$ (0.01 M), respectively. The cyclic voltammogram of **1** shows one irreversible system at $E_{pc} = -1.71$ V and two reversible systems at $E_{\frac{1}{2}} = -1.86$ and -1.91 V. In the presence of CO_2 the latter redox system exhibits a pronounced electrocatalytic current, resulting in the formation of carbon monoxide. Reaction of L with $[\{RuCl_2(CO)_2\}_n]$ in the presence of small amounts of H^+ afforded the monodentate L complex *cis*-Cl_2-*trans*-P,P-*cis*-$(CO)_2$-$[RuCl_2L_2(CO)_2]$ **3** (yield 80%). Copper(I)-induced assembly of two molecules of **3** results in the selective and quantitative formation of a 36-membered metallomacrocycle **4**. This complex exhibits a quasi-reversible oxidation at $E_{\frac{1}{2}} = 0.29$ V and an electrodeposition–redissolution redox system at $E_{pc} = -0.21$ and $E_{pa} = -0.10$ V due to formation of Cu^0 on the electrode surface. Reaction of L with $[\{RhCl(C_2H_4)_2\}_2]$ led to the (chloromethyl)-rhodium(III) complex $[RhCl_2(CH_2Cl)L]$ **5** (90%). Treatment of **5** in ethanol in the presence of silver(I) resulted in the formation of $[RhCl_2(CH_2OEt)L]$ **6** (63% yield), where the meridional arrangement of the phosphine was maintained.

The co-ordination chemistry of difunctional ligands containing both P^{III} and a N-donor is currently a topic of great interest.[1] One important feature of such hybrid ligands is their ability to form non-symmetric chelate complexes. Owing to the distinct electronic properties of the soft phosphorus and hard nitrogen centres it might be anticipated that structures containing such chelating ligands allow precise control of the co-ordination sphere during a catalytic cycle, and, in particular, facilitate the positioning and orientation of entering mono- or di-functional substrates (*trans* to P or N). One may also take advantage of the hemilabile behaviour of some *P*,*N* ligands in certain chelate complexes, *i.e.* their ability to generate by labilisation of the N-bonded fragment a free co-ordination site.[2]

Whereas most studies on *P*,*N*-ligands have been concerned with phosphino-substituted pyridines, relatively little attention has been paid to oligopyridylphosphines, notably to bipyridylphosphines.[3] The latter combine the co-ordination properties of a remarkable chelator, the bipy unit, with that of a trivalent phosphorus atom. In a preliminary account we have briefly described the synthesis of 6-(2-diphenylphosphinoethyl)-2,2′-bipyridine, L, and shown that it may display either P-monodentate behaviour **a** towards transition-metal ions or act as a bridging ligand **b** between two metal centres.[4] Mode **a** was exploited for the construction of highly organised architectures generated by assembling bipyridine units belonging to distinct metal complexes.

We now report full synthetic data for the tridentate ligand L, and for complexes of type **a** and **b** and also describe a new bonding mode of L, namely the meridional co-ordination type **c**, found in some ruthenium and rhodium complexes.

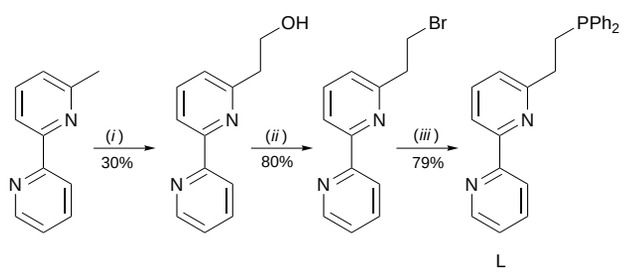

Scheme 1 Synthesis of L. (*i*) $LiNPr^i_2$, −78 °C, tetrahydrofuran (thf), anhydrous paraformaldehyde; (*ii*) HBr (33%)–$MeCO_2H$; (*iii*) $Li(PPh_2)$, −78 °C, thf

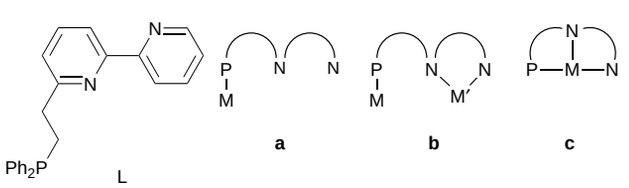

Results and Discussion

Ligand synthesis

The *P*,*N*,*N* ligand L has been obtained as a white solid in three steps from 6-methyl-2,2′-bipyridine[5] as sketched in Scheme 1. Lithiation of 6-methyl-2,2′-bipyridine with lithium diisopropylamide, at low temperature, was followed by reaction with anhydrous paraformaldehyde. After work-up the primary alcohol 6-(2-hydroxyethyl)-2,2′-bipyridine was obtained in 30%

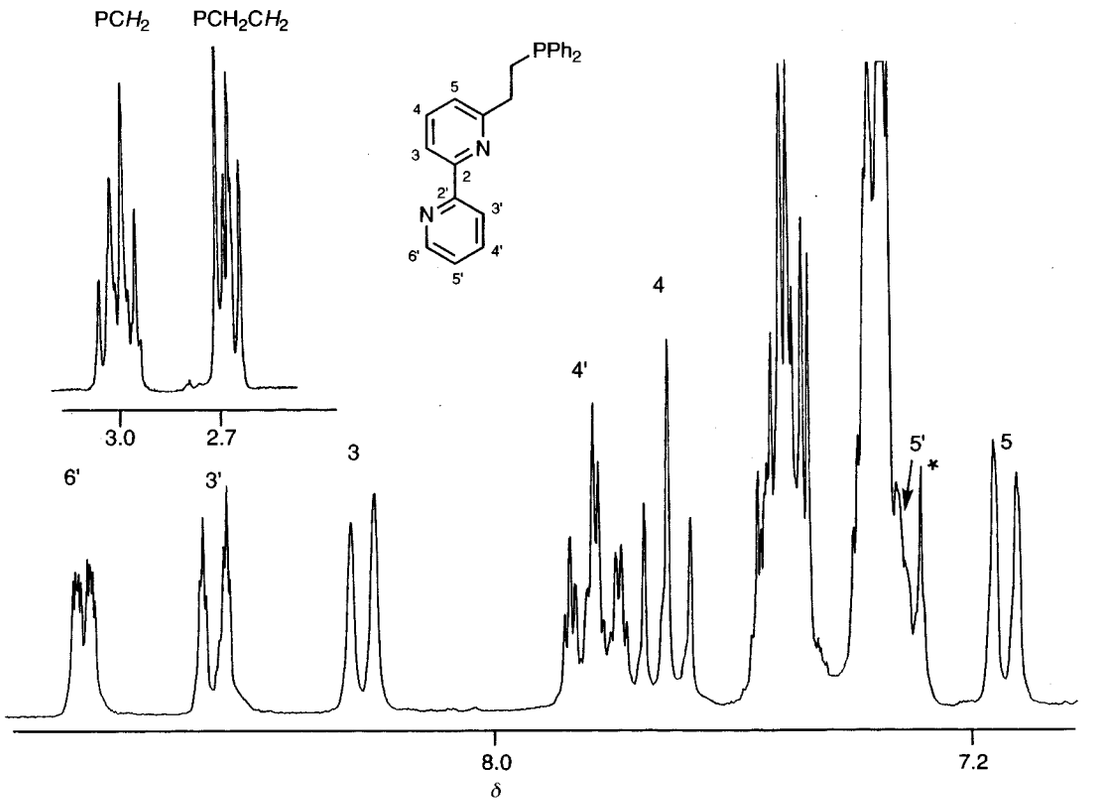

Fig. 1 Partial view of the ^{1}H NMR spectrum of L in $CDCl_3$. The peak marked with an asterisk corresponds to residual $CHCl_3$

yield. Treatment of it with HBr (33%)–$MeCO_2H$ resulted in formation of the bromo derivative in 80% yield. Further reaction with $Li(PPh_2)$ at low temperature afforded L in 79% yield. The ^{1}H NMR spectrum of this phosphine displays the expected seven bipyridine H signals in the aromatic region (Fig. 1) and an A_2B_2X [X = P, A = PCH_2, ^2J(PA) = 9 Hz] pattern for the two methylene protons. The phosphorus signal appears at δ −14.9 in the ^{31}P-{^{1}H} NMR spectrum.

Ruthenium carbonyl complexes

For the present study $[\{RuCl_2(CO)_2\}_n]$ was used as ruthenium precursor. Since this polymeric complex contains traces of acid originating from its preparation,[6] we decided first to use it in association with triethylamine. Reaction of this system with *n* equivalents of L gave a mixture of complexes **1** and **2** (Scheme 2), which were separated by flash chromatography.

The meridional arrangement of the *P*,*N*,*N* ligand in complexes **1** and **2** was inferred from a combination of IR and NMR data and confirmed in the case of **1** by an X-ray structural analysis (Fig. 2; Table 1). The ruthenium atom in **1** is in an almost octahedral environment with the two Cl atoms occupying *trans* positions [Cl(1)–Ru–Cl(2) 171.98(8)°]. The six-membered phosphorus-containing metallocycle adopts an envelope shape, the folding being about the C(11)–C(13) axis [dihedral angle between the C(11)–C(12)–C(13) and the N(2)–Ru–P planes: 64°]. This ring appears somewhat strained as shown by the rather large C(13)–C(12)–C(11) angle [114.0(8)°]. The Ru–P bond length is 2.290(2) Å and the two Ru–N distances differ only slightly [Ru–N(1) 2.122(6), Ru–N(2) 2.177(6) Å]. The meridional *P*,*N*,*N* arrangement imposes a tilt angle between the pyridine rings of 10°.

Reaction of L with $[\{RuCl_2(CO)_2\}_n]$ (L:Ru ratio $2n:n$) in methanol, at room temperature, in the absence of triethylamine resulted mainly in formation of the colourless complex **3** (80% yield), with small amounts of **1** and **2**. It is likely that during the formation of **3** transient protonation of the bipyridine moiety occurs and hence favours *P*-monodentate co-ordination. The

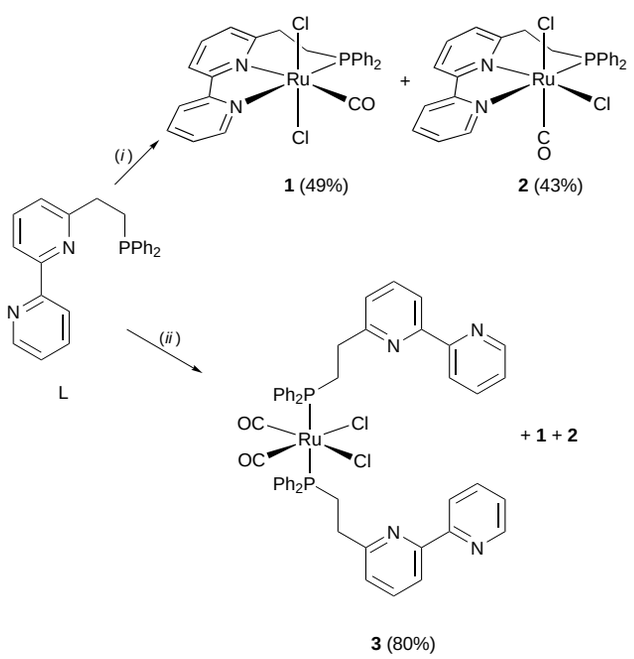

Scheme 2 (*i*) $[\{Ru(CO)_2Cl_2\}_n]$ (1 equivalent), NEt_3 (1 equivalent), MeOH, room temperature (r.t.); (*ii*) $[\{Ru(CO)_2Cl_2\}_n]$ (0.5 equivalent), MeOH, r.t.

^{31}P-{^{1}H} NMR spectrum of complex **3** displays a singlet at δ 18.2 (free phosphine δ −14.9), showing the equivalence of the two phosphorus atoms. As expected for a *trans* arrangement of the phosphine ligands, the PCH_2 groups appear as a virtual triplet in the CH_2(bipy)-decoupled ^{1}H NMR spectrum.[8] The *cis*-$(CO)_2$, *cis*-Cl_2 stereochemical arrangement in complex **3** was deduced from the presence of two ν(C=O) absorption bands (2052 and 1988 cm^{-1}) and two strong ν(Ru–Cl) stretching vibrations (299 and 285 cm^{-1}) in the IR spectrum.[9] The *trans*-P_2-*cis*-$(CO)_2$-*cis*-Cl_2 stereochemistry was confirmed by a single-crystal

X-ray diffraction study (Fig. 3) which has been previously reported.[4]

It is interesting that the tridentate behaviour of the *P*,*N*,*N* ligand in complexes **1** and **2** induces a high-field shift of the ^{31}P NMR resonances with respect to the phosphorus signal of the *P*-monodentate complex **3** (δ 47.6 **1**, 35.9 **2**, 18.2 **3**).

Electrochemical properties of complexes 1 and 2

Ruthenium complexes of the type $[Ru^{II}Cl_2(bipy)(CO)_2]$ (bipy = 2,2′-bipyridine) have recently been investigated with respect to their electrochemical properties. It was found that electrochemical reduction of *trans*-dichloro stereoisomers exclusively leads to a polymeric film of generic formula $[\{Ru(bipy)(CO)_2\}_n]$ which displays outstanding catalytic activity in the electrochemical reduction of carbon dioxide.[10,11] The formation of such organometallic polymers results from addition of two electrons to $[Ru^{II}Cl_2(bipy)(CO)_2]$ and subsequent loss of two chloride ligands. Electropolymerisation proceeds *via* transient formation of di- and tetra-meric complexes. Structural parameters such as the relative positions of the leaving groups play a crucial role in this process; interestingly, electroreduction of the *cis*-Cl_2 stereoisomers did not lead to polymer formation, but afforded dimers.[12] Extension of this electropolymerisation technique to other ruthenium carbonyl complexes is an important question.[13] The availability of complexes **1** and **2** afforded a good opportunity to study whether polymer formation still occurs when phosphine donors are present in the co-ordination sphere of the ruthenium centre.

Table 1 Selected bond lengths (Å) and angles (°) for complex **1**

Ru–P	2.290(2)	P–C(13)	1.802(9)
Ru–Cl(1)	2.383(2)	P–C(14)	1.831(8)
Ru–Cl(2)	2.407(2)	P–C(20)	1.846(7)
Ru–N(1)	2.122(6)	Ru–C(1)	1.820(8)
Ru–N(2)	2.177(6)	C(1)–O	1.144(8)
Cl(1)–Ru–Cl(2)	171.98(8)	Ru–P–C(13)	106.6(3)
P–Ru–N(1)	171.8(2)	Ru–P–C(14)	119.8(3)
N(2)–Ru–C(1)	172.8(3)	Ru–P–C(20)	121.3(2)
P–Ru–Cl(1)	93.63(7)	P–C(13)–C(12)	110.0(6)
P–Ru–Cl(2)	90.85(8)	C(13)–C(12)–C(11)	114.0(8)

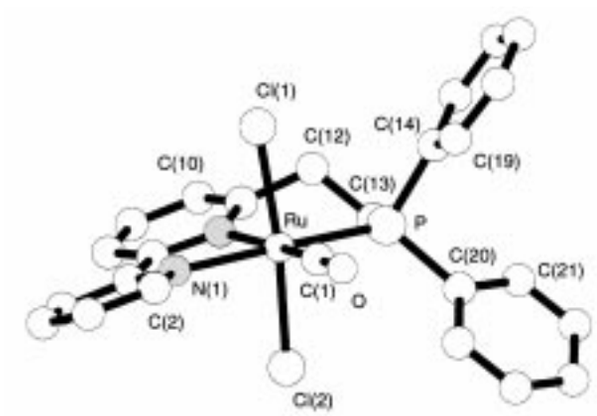

Fig. 2 A MolView[7] drawing of complex **1**

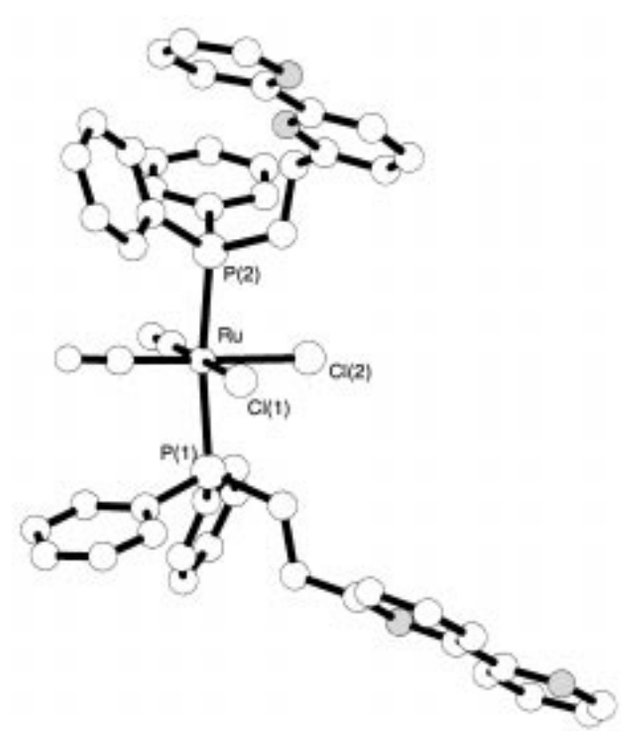

Fig. 3 A MolView[7] drawing of complex **3**

The electrochemical behaviour of complex **1** (10^{-3} M) in MeCN containing NBu_4ClO_4 (0.1 M) is illustrated by the cyclic voltammogram shown in Fig. 4. In the positive region [curve (*a*)] the complex is oxidised reversibly by a one-electron process into the corresponding ruthenium(III) species $[Ru^{III}Cl_2L(CO)]^+$ {$E_{\frac{1}{2}} = 0.80$ V, compare $E_{\frac{1}{2}} = 1.45$ V[13] for *trans*-Cl_2-$[Ru^{II}Cl_2(bipy)(CO)_2]$}. Exhaustive oxidation at 1.00 V with subsequent reduction at 0.60 V regenerated quantitatively the initial complex. This result shows that $[Ru^{III}Cl_2L(CO)]^+$ is stable, unlike $[Ru^{III}Cl_2(bipy)(CO)_2]^+$ which readily undergoes substitution of one chloride and one CO under similar conditions.[14] The visible absorption spectrum of $[Ru^{III}Cl_2L(CO)]^+$ displays absorption bands at 614 (ε = 1300) and 474 nm (ε = 1200 M^{-1} cm^{-1}) while that of the initial complex lies at 400 nm (ε = 1000 M^{-1} cm^{-1}).

In the cathodic area the voltammogram exhibits a first irreversible system ($E_{pc} = -1.71$ V) followed by two quasi-reversible ones ($E_{\frac{1}{2}} = -1.86$ and -1.91 V) [Fig. 4, curve (*b*)]. In contrast to the observations made for *trans*-Cl_2-$[RuCl_2(bipy)(CO)_2]$,[9] controlled-potential electrolysis of complex **1** at -1.70 V did not produce any polymeric electroactive film on the working electrode. Indeed, after one electron per molecule of complex was consumed a pale yellow solution was obtained, characterised by a broad absorption between 340 and 500 nm. Similar results were obtained using NMe_4BF_4 (0.05 M in acetonitrile) as supporting electrolyte. After the one-electron electrolysis was complete the solvent was evaporated and the residue extracted with dichloromethane. The solution IR spectrum showed a unique absorption band in the carbonyl region (at 1927 cm^{-1}). Mass spectroscopy [desorption chemical ionisation (DCI) electron-capture mode] unambiguously revealed the presence of an intense peak corresponding to $[Ru^{I}Cl(L)(CO)(MeCN)]$ (*m*/*z* 574). This complex was likely formed according to following two-step mechanism in equations (1) and (2).

$$[Ru^{II}Cl_2L(CO)] + e^- \longrightarrow [Ru^{II}Cl_2(L^{\bullet -})(CO)] \quad (1)$$

$$[Ru^{II}Cl_2(L^{\bullet -})(CO)] + MeCN \longrightarrow [Ru^{I}Cl(L)(CO)(MeCN)] + Cl^- \quad (2)$$

The cyclic voltammogram of a solution containing the electrochemically generated complex $[Ru^{I}Cl(L)(CO)(MeCN)]$ exhibits the two successive reversible systems at $E_{\frac{1}{2}} = -1.86$ and -1.91 V described above. Exhaustive electrolysis carried out at -1.85 V, in MeCN containing NBu_4ClO_4 (0.1 M), consumes one electron per molecule and produces a *deep green* solution (λ_{max} 386, 520, 580 and 750 nm), suggesting[12] the formation of a dimeric complex according to the process described in equations (3)–(5).

$$[Ru^{I}Cl(L)(CO)(MeCN)] + e^- \longrightarrow [Ru^{I}Cl(L^{\bullet -})(CO)(MeCN)] \quad (3)$$

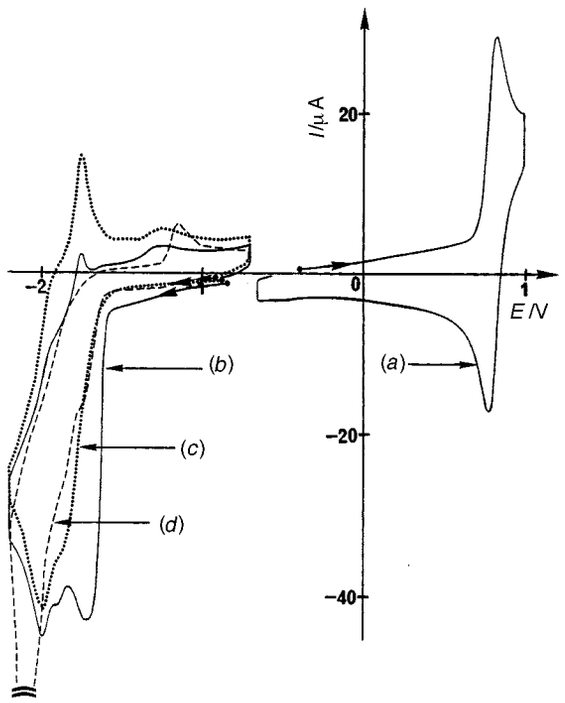

Fig. 4 Cyclic voltammograms at a vitreous carbon electrode (19.6 mm^2), in a MeCN solution containing NBu_4ClO_4 (0.1 M) and complex **1** (1 mM), $\nu = 100$ mV s^{-1}. Initial solution (*a*) between −0.65 and +1.00 V, (*b*) between −0.70 and −2.20 V, (*c*) solution after exhaustive reduction at −1.70 V, under Ar and (*d*) under CO_2

$$[Ru^{I}Cl(L^{\bullet -})(CO)(MeCN)] \rightleftharpoons [Ru^{0}L(CO)(MeCN)] + Cl^{-} \quad (4)$$

$$[Ru^{0}L(CO)(MeCN)] \rightleftharpoons \tfrac{1}{2}[\{Ru^{0}L(CO)(MeCN)\}_2] \quad (5)$$

After quantitative formation of the dimeric species, the cyclic voltammogram [Fig. 4, curve (*c*)] only shows the second reversible system ($E_{\frac{1}{2}} = -1.91$ V) which corresponds to the reduction of the dimer. In view of the quasi-reversibility of the system at −1.86 V in the initial voltammogram, it is likely that dimer formation occurs slowly on the experimental time-scale.

The cyclic voltammogram under CO_2 of the ruthenium(I) complex obtained at −1.70 V *vs.* $Ag–Ag^+$ (0.01 M) is shown in Fig. 4, curve (*d*). The first reduction (dimer formation, at −1.86 V) remains unaffected, while the second reduction peak, at $E_{pc} = -1.97$ V, shows a strong enhancement of the cathodic current. This is a clear indication that the first reduction of the resulting dimer leads to an electrocatalyst for the reduction of CO_2. A GC analysis after an electrocatalysis at −1.85 V in MeCN–NBu_4ClO_4 (0.1 M)–water (10% v/v) revealed the formation of carbon monoxide (faradic yield 14%). However, molecular hydrogen was formed as main product as a consequence of the strong cathodic potential. Note that during the reduction no formate was detected. Obviously, the high cathodic potential of the system [$E \approx -1.80$ V, Fig. 4, curve (*d*)] makes this ruthenium dimer less attractive for electrocatalytic production of CO from CO_2 than the polymeric $[\{Ru^{0}(bipy)(CO)_2\}_n]$ film (100% faradic yield at −1.2 V *vs.* saturated calomel electrode, SCE, in water).[10,11]

The *cis*-Cl_2 isomer **2** presents essentially the same electrochemical behaviour as that of complex **1**, involving similar redox processes. The formation of the corresponding $[Ru^{I}Cl(L)(CO)(MeCN)]$ complex occurs at −1.83 V, while the quasi-reversible dimerisation lies at $E_{\frac{1}{2}} = -1.78$ V and the resulting dimer is reversibly reduced at $E_{\frac{1}{2}} = -1.94$ V. On the other hand, the reversible one-electron oxidation of **2** leading to $[Ru^{III}Cl_2L(CO)]^+$ is observed at a more anodic potential ($E_{\frac{1}{2}} = 1.04$ V) than that of the *trans*-Cl_2 isomer **1** ($E_{\frac{1}{2}} = 0.80$ V).

In summary, this electrochemical study reveals that during the two electron-reduction process of complex **1** a ruthenium(0) dimer is formed, thus contrasting with the behaviour of *trans*-Cl_2-$[RuCl_2(bipy)(CO)_2]$ which leads to formation of a ruthenium(0) polymeric species. This difference possibly arises from the steric bulk of the phosphino fragment preventing polymerisation of the reduced species. This interpretation must however be regarded with care since isomerisation of the electrochemically generated species $[Ru^{I}Cl(L)(CO)(MeCN)]$ (or its reduced form) might occur and hence result in formation of a species with *cis*-located leaving groups, a stereochemical arrangement not favourable for polymerisation.[12]

Mixed ruthenium(II)–copper(I) complex

Complex **3** possesses two free bipyridine subunits located at the two ends. Clearly, the large separation between these two free binding sites and the rigidity of the P–Ru–P spacer disfavours complexation of both bipyridines around an additional single metal centre. The co-ordinative properties of this ditopic metallo-synthon were investigated towards the Cu^+ cation.

Stoichiometric mixing of complex **3** with $[Cu(MeCN)_4]ClO_4$[15] yielded quantitatively the deep red complex **4** ($\lambda_{max} = 442$ nm, $\varepsilon = 14\,300$ M^{-1} cm^{-1}). The positive-ion FAB mass spectrum of the resulting complex gave an intense peak at *m*/*z* 2158.9 [$M - ClO_4$] with the expected isotopomer distributions and no significant peaks at higher mass. The self-assembled complex **4** is best described as a 36-membered $Ru_2Cu_2P_4N_8$ metallomacrocycle as confirmed by a crystal structure determination (Scheme 3 and Fig. 5).[4]

The IR (ν_{CO} 2050 and 1987 cm^{-1}), far-IR [ν(Ru–Cl) 304 and 280 cm^{-1}], and NMR spectroscopic data are similar to those observed for precursor **3**, in full accord with the fact that the *trans*-P,P-*cis*-$(CO)_2$-*cis*-Cl_2 stereochemistry around the Ru is maintained in the tetrametallic complex **4**. A remarkable feature of this reaction is that no polymer formation was observed. Furthermore, it is noteworthy that the copper-controlled assembly of bipyridine units results selectively in a non-helical arrangement (**d**). Similar observations were recently made with purely organic bis(bipyridine) compounds and steric effects have been postulated to play a major role in the formation of the side-by-side non-helical isomer (**d**).[16]

Electrochemical properties of complexes 3 and 4

Complex **3** exhibits a unique irreversible redox process located at a large cathodic potential ($E_{pc} = -2.14$ V). Exhaustive electrolysis carried out at −2.20 V involves two electrons per mol of complex and leads to decomposition of the reduced species. The cyclic voltammogram obtained after this exhaustive reduction showed the typical reversible one-electron reduction signal of free L ($E_{\frac{1}{2}} = -2.54$ V).

In the mixed Ru_2Cu_2 complex **4** the $Cu^{II/I}$ redox system appears as quasi-reversible ($E_{\frac{1}{2}} = 0.29$ V), while a typical electrodeposition–redissolution peak system due to copper(0) formation at the working electrode surface is obtained ($E_{pc} = -0.21$ V, $E_{pa} = -0.10$ V).[17]

Rhodium complexes

Since L is suitable for meridional co-ordination, we surmised that it would also display tridentate behaviour in square-planar complexes. We therefore investigated its co-ordinative properties towards rhodium(I).

Treatment of $[\{RhCl(C_2H_4)_2\}_2]$ with 2 equivalents of L in dichloromethane resulted in the formation of a pale yellow, sparingly soluble species (yield 90%) which was characterised by elemental analysis, mass spectrometry, ^{31}P and ^{1}H NMR spectroscopies. Its ^{31}P NMR spectrum displays a doublet at δ 28.3 [J(RhP) = 123 Hz]. The ^{1}H NMR spectrum exhibits signals

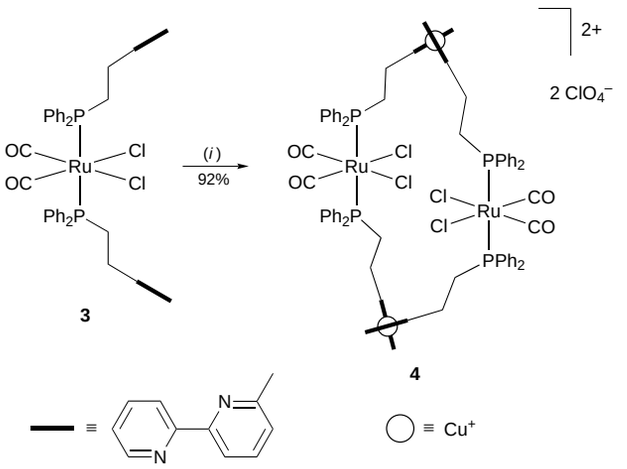

Scheme 3 (*i*) $[Cu(MeCN)_4]ClO_4$, MeCN–CH_2Cl_2 (1 : 1), r.t.

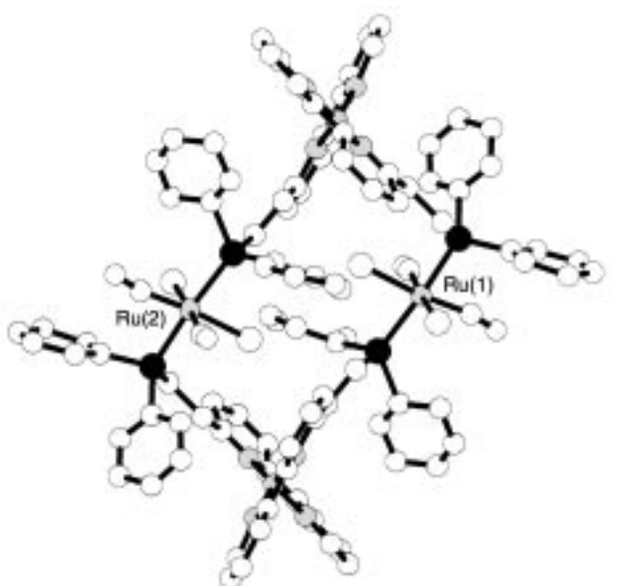

Fig. 5 A MolView[7] drawing of complex **4**

characteristic of the PCH_2CH_2 moiety [two complex multiplets (2 H : 2 H), at δ 3.5 and 2.8] and a well resolved ABXY spin system (δ_A 4.1 and δ_B 3.7, X = P, Y = Rh, intensity 1 : 1), consistent with a metal-bound CH_2R group. The formation of a chloromethyl complex was confirmed by the FAB mass spectrum which shows an intense peak at *m/z* 555.0 (intensity 100%, expected isotopic profile), corresponding to a $[RhCl(CH_2Cl)L]^+$ cation. A fragmentation peak (at *m/z* 506.0, intensity 35%) corresponding to the loss of a 'CH_2Cl' fragment was also detected. These results are consistent with the formula drawn for complex **5** (Scheme 4).

It is likely that reaction between ligand L and the rhodium(I) ethylene complex generates the electron-rich $[Rh^ICl(L)]$ intermediate which in turn undergoes facile oxidative addition of methylene chloride affording the rhodium(III) complex **5**. Dichloromethane activation by rhodium(I) phosphine complexes has previously been observed.[18]

Nucleophilic substitution at the chloromethyl fragment in complex **5** by EtOH was achieved using AgO_3SCF_3 and afforded the highly soluble yellow complex **6** (Scheme 4). It is noteworthy that no reaction occurs with ethanol in the absence of silver salt. The phosphorus resonance of complex **6** appears at δ 27.7 [*J*(RhP) = 132 Hz] (*cf.* δ 28.3 for **4**). The ^1H NMR spectrum exhibits signals corresponding to an ethyl group, two multiplets for the PCH_2CH_2 spacer and an ABX pattern (X = Rh) for the Rh–CH_2OEt hydrogens. The co-ordinated methylene resonates at δ 72.0 [*J*(CRh) = 17 Hz] in the ^{13}C-{^1H}

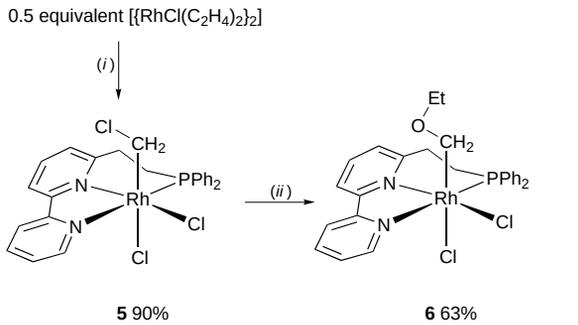

Scheme 4 (*i*) L (1 equivalent), CH_2Cl_2; (*ii*) AgO_3SCF_3 (1 equivalent), EtOH

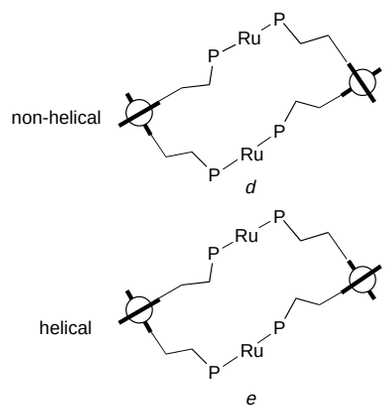

NMR spectrum. The FAB mass spectrum shows an intense peak at *m/z* 565.1 (intensity 100%) corresponding to the $[RhCl(CH_2OEt)L]^+$ cation (expected isotopic profile) and a fragment of mass 506.1 (intensity 40%) due to the loss of the 'CH_2OEt' ligand. Although the monocrystals obtained for **6** were of poor quality,† X-ray diffraction data clearly confirmed the proposed meridional arrangement of the tridentate ligand and the *cis* dichloro configuration.

Conclusion

In this study three co-ordination modes were found for the tridentate L ligand. An example of monodentate behaviour was found in *cis*-Cl_2-*cis*-$(CO)_2$-*trans*-P,P-$[RuCl_2(CO)_2L_2]$ **3**, a complex where the RuP_2 fragment plays the role of a rigid spacer between two well separated bipyridine units. The whole complex **3** can be regarded as a multisite metallo-synthon suitable for the preparation of highly organised architectures. This is illustrated by the 36-membered metallomacrocycle **4** in which the L ligand behaves as a non-symmetric linker between a ruthenium(II) and a copper(I) centre. Tridentate-meridional co-ordination was observed in the chlororuthenium(II) carbonyl complexes **1** and **2** and in the rhodium(III) species **5** and **6**. In contrast to *trans*-Cl_2-$[RuCl_2(bipy)(CO)_2]$, the electrochemical reduction of the ruthenium(II) complex **1** does not generate a polymer, but a dimeric species, suggesting that the bulky phosphine controls the transformation of the species obtained after a two-electron reduction. The electrogenerated dimer is active towards the reduction of carbon dioxide to carbon monoxide, but at much lower cathodic potential than for the above-mentioned polymer.

The electron-rich rhodium(I) intermediate obtained by treating the *P*,*N*,*N* ligand with $[\{RhCl(C_2H_4)_2\}_2]$ results in activation of dichloromethane under ambient conditions. Chemical transformation of the co-ordinated 'CH_2Cl' fragment maintains the

† Crystal data: orthorhombic, space group *Pbca*, *a* = 11.915(6), *b* = 14.55(2), *c* = 29.77(2) Å.

meridional *P*,*N*,*N* co-ordination of the ligand, emphasising its potential role as an ancillary ligand for further stereocontrolled reactions.

Experimental

Nuclear magnetic resonance spectra were recorded on Bruker SY-200 or AC-200 instruments at room temperature and at 200.1 MHz for ^{1}H, 50.3 MHz for ^{13}C, and 81.0 MHz for ^{31}P. The ^{1}H NMR chemical shifts are reported in parts per million (ppm) relative to residual protiated solvents (δ 7.26 for $CDCl_3$, 2.04 for [$^2H_6$]acetone, and 1.94 for CD_3CN); ^{13}C-{^{1}H} NMR chemical shifts are reported relative to $CDCl_3$ (δ 77.03), [$^2H_6$]acetone (δ 206.00, 29.80) and CD_3CN (δ 181.21, 1.32) while ^{31}P-{^{1}H} NMR chemical shifts are given relative to external 85% H_3PO_4. Infrared spectra were recorded with an IFS 25 Bruker spectrometer, with the sample in the form of anhydrous KBr pellets. Fast atomic bombardment (FAB, positive mode) spectra were recorded on a ZAB-HF-VB-analytical apparatus in *m*-nitrobenzyl alcohol matrices; Ar atoms were used for the bombardment (8 keV; eV ≈ 1.60 × 10^{-19} J). The DCI (electron-capture mode) mass spectra were obtained on an AEI Kratos MS 50 spectrometer fitted with an ION Tech Ltd. gun. Routine absorption spectra were measured in acetonitrile solutions at room temperature with a Uvikon 941 spectrophotometer, electronic absorption spectra of electrolysed solutions on a Hewlett-Packard HP 8452A diode-array spectrophotometer controlled by a Compaq 286 computer equipped with a Citizen 120D printer. Structural assignments are based on ^{1}H, ^{13}C-{^{1}H}, ^{31}P-{^{1}H} NMR, IR, and positive-ion FAB mass spectra, and elemental analysis. All reactions were carried out under dry argon by using Schlenk-tube and vacuum-line techniques. Solvents, including $CDCl_3$, were dried over suitable and freshly distilled under argon before use. The LiBu^n solutions were titrated according to ref. 19. [{$RuCl_2(CO)_2$}$_n$] was prepared according to ref. 6.

Crystallography

Crystal data for complex 1. $C_{25}H_{21}Cl_2N_2OPRu$, $M = 568.41$, gold-yellow crystals (0.12 × 0.20 × 0.25 mm), monoclinic, space group $P2/c$ with $a = 13.215(7)$, $b = 15.572(6)$, $c = 11.581(6)$ Å, $\beta = 100.63(6)°$, $U = 2342(2)$ Å^3, $Z = 4$, $D_c = 1.612$ g cm^{-3}, $F(000) = 1144$, $\mu = 9.74$ cm^{-1}.

A suitable crystal was obtained by slow diffusion of hexane into a dichloromethane solution of complex **1** at room temperature. Data were collected on an Enraf-Nonius CAD4 diffractometer at room temperature with graphite-monochromated Mo-Kα radiation (λ = 0.7107 Å). The cell parameters were obtained by fitting a set of 25 high-θ reflections. The data collection [ω–2θ scan type, $2\theta_{max} = 50°$, ranges *h* 0–15, *k* 0–18, *l* −13 to 13, intensity controls without appreciable decay (0.2%)] gives 4481 reflections from which 2017 were independent ($R_{int} = 0.025$) with $I > 3\sigma(I)$. After Lorentz-polarisation corrections, the structure was solved by a Patterson map which revealed the ruthenium atom. The remaining non-hydrogen atoms were found after several scale-factor and Fourier-difference calculations. After isotropic ($R = 0.095$) refinement, an absorption correction (maximum 1.5344, minimum 0.7763) was made using DIFABS.[20] After anisotropic refinement ($R = 0.065$), all hydrogen atoms were found with a Fourier-difference map (between 0.59 and 0.27 e Å^{-3}). The whole structure was refined by full-matrix least squares on F {x, y, z, β_{ij} for Ru, P, Cl, N, C and O atoms and x, y, x for H atoms; 353 variables and 2017 observations; $w = 1/\sigma(F_o)^2 = [\sigma^2(I) + (0.04F_o^2)^2]^{\frac{1}{2}}$} with the resulting $R = 0.039$, $R' = 0.035$ and $S = 2.30$ (residual $\Delta\rho \leqslant 0.58$ e Å^{-3}). Atomic scattering factors were from ref. 21. All calculations were performed on a Digital MicroVAX 3100 computer with the MOLEN[22] package.

CCDC reference number 186/642.

Electrochemical instrumentation and procedures

Acetonitrile (Rathburn, HPLC grade) was used as received. Tetrabutylammonium perchlorate from Fluka was recrystallised from ethyl acetate and dried under vacuum at 80 °C for 3 d. Tetramethylammonium tetrafluoroborate from Fluka was dried under vacuum at 80 °C for 3 d. Electrochemical experiments were carried out using a Princeton Applied Research potentiostat-galvanostat (model 273) equipped with a Sefram TGM 164 X-Y recorder. Potentials are relative to the Ag–Ag$^+$ (0.01 M) electrode in MeCN containing NBu_4ClO_4 (0.1 M). Working electrodes for cyclic voltammetry consisted of a vitreous carbon disc (5 mm diameter) polished with 2 μm diamond paste. All experiments were run in a conventional three-electrode cell in a dry-box (Jaram) under an argon atmosphere. Exhaustive electrolyses were carried out with a 5 cm^2 platinum electrode.

Preparations

6-(2-Hydroxyethyl)-2,2′-bipyridine. A hexane solution of LiBu^n, titrated at 1.51 M (19.9 cm^3, 0.030 mol), was added dropwise to a solution of diisopropylamine (3.200 g, 0.032 mol) in thf (25 cm^3) at −78 °C. After 1 h a solution of 6-methyl-2,2′-bipyridine (5.106 g, 0.030 mol) in thf (25 cm^3) was added over 10 min. The solution immediately turned deep blue, indicative of fast metallation. After 3 h anhydrous paraformaldehyde (1.080 g, 0.036 mol) was added as a solid and, after stirring for 5 h at −78 °C, the temperature was allowed to rise to room temperature. The solution was hydrolysed with water (1 cm^3) presaturated with NH_4Cl before the solvent was removed by rotary evaporation. The crude product was dispersed on alumina and purified by column chromatography, eluting first with CH_2Cl_2–hexane (1 : 1) (recovering unchanged starting product, 1.9 g) and then with 2% MeOH in CH_2Cl_2 affording the analytically pure required compound **2** ($R_f = 0.23$; 1.8 g, 30%). ^{1}H NMR ($CDCl_3$): δ 8.50 (m, 1 H, H$^{6'}$), 8.08 (m, 2 H, H$^{3,3'}$), 7.57 (m, 2 H, H$^{4,4'}$), 7.05 (m, 2 H, H$^{5,5'}$), 4.74 (s br, 1 H), 3.96 (s br, 2 H, CH_2O) and 2.93 [m, 2 H, CH_2(bipy)]. ^{13}C-{^{1}H} NMR ($CDCl_3$): δ 159.35 (C_q), 155.48 (C_q), 154.82 (C_q), 148.73 (CH), 137.12 (CH), 136.59 (CH), 123.36 (CH), 123.21 (CH), 120.61 (CH), 118.55 (CH), 61.33 (CH_2O) and 39.12 [CH_2(bipy)]. Mass spectrum: *m*/*z* 200 (100%) (Found: C, 71.85; H, 5.87; N, 13.91. Calc. for $C_{12}H_{12}N_2O$: C, 71.98; H, 6.04; N, 13.99%).

6-(2-Bromoethyl)-2,2′-bipyridine. The above alcohol (1.8 g, 9.0 mmol) was treated with HBr (33%)–$MeCO_2H$ (25 cm^3) at 100 °C during 18 h. After cooling the reaction mixture to room temperature, cold water (50 cm^3) was added carefully and the resultant solution neutralised with aqueous NaOH (10%) solution. The yellowish oil so obtained was extracted with CH_2Cl_2 (3 × 50 cm^3) and the organic phases were dried over anhydrous Na_2SO_4. The crude compound was purified through a flash chromatography column packed with silica and eluted with CH_2Cl_2 containing 0.2 to 0.5% MeOH ($R_f = 0.63$, alumina, CH_2Cl_2) affording the analytically pure compound (1.9 g, 80%). ^{1}H NMR ($CDCl_3$): δ 8.64 [ddd, 1 H, H$^{6'}$, ^3J(HH) = 4.7, ^4J(HH) = 1.8, ^5J(HH) = 0.8], 8.43 [dm, 1 H, H$^{3'}$, ^3J(HH) = 7.9], 8.26 [dd, 1 H, H^3, ^3J(HH) = 7.2, ^4J(HH) = 0.8], 7.75 [ddd, 1 H, H$^{4'}$, ^3J(HH) = 7.9, ^3J(HH) = 7.5, ^4J(HH) = 2.9], 7.70 [t, 1 H, H^4, ^3J(H^{4}H^3) = ^3J(H^{4}H^5) = 7.9], 7.24 [ddd, 1 H, H$^{5'}$, ^3J(HH) = 4.8, ^3J(HH) = 7.6, ^4J(HH) = 1.3], 7.14 [dd, 1 H, H^5, ^3J(HH) = 7.7, ^4J(HH) = 0.9], 3.85 [t, 2 H, CH_2Br, ^3J(HH) = 6.9] and 3.37 [t, 2 H, CH_2(bipy), ^3J(HH) = 7.1 Hz]. ^{13}C-{^{1}H} NMR ($CDCl_3$): δ 157.59 (C_q), 156.02 (C_q), 155.70 (C_q), 148.99 (CH), 137.16 (CH), 136.68 (CH), 123.56 (CH), 123.23 (CH), 121.02 (CH), 118.97 (CH), 41.01 (CH_2Br) and 31.46 [CH_2(bipy)]. Mass spectrum: *m*/*z* 264/262 (4) and 183 (100%) (Found: C, 54.68; H, 4.03; N, 10.57. Calc. for $C_{12}H_{11}BrN_2$: C, 54.77; H, 4.21; N, 10.65%).

Compound L. A hexane solution of LiBu^n, titrated at 1.51 M (2.42 cm^3, 3.66 mmol), was added dropwise to a solution of PPh_2H (0.682 g, 3.66 mmol) in anhydrous thf (30 cm^3) at −78 °C. After 15 min the orange-red solution thus obtained was transferred dropwise *via* a cannula to a solution of 6-(2-bromoethyl)-2,2′-bipyridine (0.964 g, 3.66 mol) in thf (50 cm^3). During addition the temperature of the solution was maintained at −78 °C and the orange coloration of the Ph_2P^- anion immediately disappeared, showing fast nucleophilic substitution of the bromide. Overnight the temperature was allowed to reach room temperature before the solution was evaporated to dryness on a vacuum line. The residue was dissolved in deoxygenated CH_2Cl_2 and the suspension filtered over neutral alumina (LiBr elimination). The analytically pure ligand L was obtained by crystallisation from a CH_2Cl_2–hexane solution at −30 °C (R_f = 0.62, alumina, CH_2Cl_2–hexane 9 : 1, 1.055 g, 79%). ^{1}H NMR ($CDCl_3$): δ 8.69 [ddd, 1 H, H$^{6'}$, ^3J(HH) = 4.8, ^4J(HH) = 1.0, ^5J(HH) = 0.8], 8.51 [dm, 1 H, H$^{3'}$, ^3J(HH) = 7.6], 8.28 [dm, 1 H, H^3, ^3J(HH) = 7.9], 7.79 [td, 1 H, H$^{4'}$, ^3J(H$^{4'}$H$^{5'}$) = ^3J(H$^{4'}$H$^{3'}$) = 7.6, ^4J(HH) = 1.3], 7.69 [t, 1 H, H^4, ^3J(H^{4}H^3) = ^3J(H^{4}H^5) = 7.8], 7.59–7.35 (10 H, PPh_2), 7.27 (m, 1 H, H$^{5'}$), 7.12 [d, 1 H, H^5, ^3J(HH) = 7.6 Hz], 3.05 (δ_A) and 2.69 (δ_B) [two multiplets of an A_2B_2X system, with A = PCH_2, ^2J(PA) = 9 Hz and B = PCH_2CH_2, 4 H]. ^{13}C-{^{1}H} NMR ($CDCl_3$): δ 160.88 [d, C_qP, ^2J(CP) = 13], 156.27 (C_q, bipy), 155.41 (C_q, bipy), 148.91 (C_q, bipy), 138.61–118.32 (aromatic C), 34.40 [d, CH_2P, J(CP) = 17] and 27.67 [d, CH_2(bipy), ^2J(CP) = 13 Hz]. ^{31}P-{^{1}H} NMR ($CDCl_3$): δ −14.9. Fourier-transform IR (KBr pellet): $\tilde{\nu}$/cm^{-1} 2925m, 1571s, 1425s, 1095s, 740vs and 693vs. EI mass spectrum: *m*/*z* 384.1 (L + O) (Found: C, 78.15; H, 5.60; N, 7.51. Calc. for $C_{24}H_{21}N_2P$: C, 78.24; H, 5.75; N, 7.60%).

Complexes 1 + 2. A solution of compound L (0.210 g, 0.570 mmol) in MeOH (25 cm^3) was added to a stirred solution of [{$RuCl_2(CO)_2$}$_n$] (0.150 g, 0.657 mmol) in anhydrous MeOH (5 cm^3) adjusted to pH *ca*. 7 with triethylamine. During the course of reaction at room temperature the solution turned deep yellow. After 2 d, the solvent was removed by rotary evaporation. The crude product was purified through a flash chromatography column packed with silica, previously deactivated by treatment with triethylamine (10% in dichloromethane), and eluted with dichloromethane; R_f = 0.46 for complex **1** and 0.26 for **2** (dichloromethane). Recrystallisation of the compounds by slow evaporation of a dichloromethane–hexane solution afforded the analytically pure gold-yellow complex **1** (0.160 g, 49%) and the analytically pure lemon-yellow complex **2** (0.140 g, 43%).

Complex 1. ^{1}H NMR ($CDCl_3$) δ 9.48 (m, 1 H), 8.10 (m, 2 H), 7.90 (m, 2 H), 7.77 (m, 6 H), 7.52 (m, 2 H), 7.37 (m, 4 H), 3.58 (m, 2 H) and 2.93 (m, 2 H); ^{13}C-{^{1}H} NMR ($CDCl_3$) δ 162.73 (C_q), 155.22 (C_q), 153.13 (CH, bipy), 138.85 (CH, bipy), 137.66 (CH, bipy), 133.00 [d, *o*-C of Ph, ^2J(CP) 11], 130.03 (s, *p*-C of Ph), 128.12 [d, *m*-C of Ph, ^3J(CP) 7], 126.85 (CH bipy), 126.28 (CH of bipy), 123.00 (CH of bipy), 120.90 (CH of bipy), 32.38 [CH_2(bipy)] and 21.13 [d, CH_2P, J(CP) 28 Hz]; ^{31}P-{^{1}H} NMR (acetone + 10% [$^2H_6$]acetone) δ + 47.6; IR (KBr) $\tilde{\nu}$/cm^{-1} 3051.5w, 2956.1w, 1943s (CO), 1601.9m, 1455.8m, 1434.7m and 1103.4m; far IR 329s (Ru–Cl); positive-ion FAB mass spectrum: *m*/*z* 568.0 (M^+, expected isotopic profile) and 533.1 (M − Cl) (Found: C, 52.63; H, 3.54; N, 4.78. Calc. for $C_{25}H_{21}Cl_2N_2OPRu$: C, 52.83; H, 3.72; N, 4.93%).

Complex 2. ^{1}H NMR ($CDCl_3$) δ 9.37 (m, 1 H), 8.00 (m, 2 H), 7.75 (m, 2 H), 7.68 (m, 6 H), 7.45 (m, 2 H), 7.28 (m, 4 H), 3.48 (m, 2 H) and 2.85 (m, 2 H); ^{13}C-{^{1}H} NMR ($CDCl_3$) δ 163.58 (C_q), 157.54 (C_q), 155.23 (CH of bipy), 140.56 (CH of bipy), 138.66 (CH of bipy), 129.23 [d, *o*-C of Ph, ^2J(CP) 11], 129.25 (s, *p*-C of Ph), 129.36 [d, *m*-C of Ph, ^3J(CP) 8], 125.89 (CH of bipy), 126.03 (CH of bipy), 124.58 (CH of bipy), 120.86 (CH of bipy), 35.26 [CH_2(bipy)] and 22.12 [d, CH_2P, J(CP) 27 Hz]; ^{31}P-{^{1}H} NMR ([$^2H_6$]acetone–acetone 1 : 9) δ +35.9; IR (KBr) $\tilde{\nu}$/cm^{-1} 2929.2m, 1951.0s (CO), 1726.1m, 1456.9m, 1263.0m and 1103.6s; far IR 299s and 286s (Ru–Cl); positive-ion FAB mass spectrum: *m*/*z* 568.0 (M^+, expected isotopic profile), 540.0 (M − CO), 533.1 (M − Cl), 504.1 (M − CO − Cl − H) and 497.1 (M − 2Cl − H) (Found: C, 52.59; H, 3.43; N, 4.67. Calc. for $C_{25}H_{21}Cl_2N_2OPRu$: C, 52.83; H, 3.72; N, 4.93%).

Complex 3. A solution of compound L (0.223 g, 0.65 mmol) in MeOH (20 cm^3) was added to a stirred solution of [{$RuCl_2(CO)_2$}$_n$] (0.070 g, 0.307 mmol) in anhydrous MeOH (20 cm^3) at room temperature. During the course of reaction a white precipitate was formed. After 24 h the solvent was removed by rotary evaporation. The crude product was purified through a chromatography column packed with silica, previously deactivated by treatment with triethylamine (10% in dichloromethane), and eluted with dichloromethane; R_f = 0.65 (dichloromethane). Recrystallisation of the precipitate by slow evaporation of a dichloromethane–hexane solution afforded the analytically pure colourless complex **3** (0.233 g, 80%). UV/VIS (MeCN) λ_{max}/nm (ε/dm^3 mol^{-1} cm^{-1}): 283 (21 200) and 224 (19 900). ^{1}H NMR (CD_2Cl_2): δ 8.62 [d, 1 H, ^3J(HH) = 4.7], 8.46 [d, 1 H, ^3J(HH) = 8.0], 8.17 [d, 1 H, ^3J(HH) = 8.0], 7.93 (m, 4 H), 7.81 [t of d, 1 H, ^3J(HH) = 7.8, ^4J(HH) = 1.8], 7.63 [t, 1 H, ^3J(HH) = 7.8], 7.50 (m, 6 H), 7.29 (m, 1 H), 7.00 [d, 1 H, ^3J(HH) = 7.6 Hz], 3.51 (m, 4 H) and 2.75 (m, 4 H). ^{13}C-{^{1}H} NMR ($CDCl_3$): δ 192.47 [d, Ru–CO, ^2J(CP) = 11], 159.87 (C_q, phosphine), 156.33 (C_q, bipy), 155.43 (C_q, bipy), 148.95 (C_q, bipy), 137.16–118.49 ($C_{aromatic}$), 31.75 [s, CH_2(bipy)] and 23.29 [pseudo t, CH_2P, J(CP) = 14.5 and 13.2 Hz (^1J and ^3J not assigned)]. ^{31}P-{^{1}H} NMR ([$^2H_6$]acetone–acetone 1 : 9): δ +18.2. Fourier-transform IR (KBr pellet): $\tilde{\nu}$/cm^{-1} 3054w, 2052s (ν_{CO}), 1988s (ν_{CO}), 1579m, 1431m, 1133m, 1104m, 299 [ν(Ru–Cl)] and 285 [ν(Ru–Cl)]. Positive-ion FAB mass spectrum: *m*/*z* 964.9 ([M + H]$^+$, expected isotopic profile) (Found: C, 62.09; H, 4.14; N, 5.73. Calc. for $C_{50}H_{42}Cl_2N_4O_2P_2Ru$: C, 62.24; H, 4.39; N, 5.81%).

Complex 4. A solution of $[Cu(MeCN)_4]ClO_4$ (0.020 g, 0.060 mmol) in anhydrous MeCN (10 cm^3) was added at room temperature, under argon, to a stirred solution of complex **3** (0.058 g, 0.060 mmol) in anhydrous CH_2Cl_2 (15 cm^3). During addition the solution turned deep red, showing fast copper(I) complexation. After 8 h it was filtered over Celite and evaporated to dryness. Slow evaporation of a MeCN–toluene solution of the crude product led to the analytically pure cherry-red complex **4** (0.062 g, 92%). UV/VIS (MeCN) λ_{max}/nm (ε/dm^3 mol^{-1} cm^{-1}): 442 (14 300), 292 (138 000), 260 (127 000) and 213 (153 000). ^{31}P-{^{1}H} NMR (CD_3CN): δ +19.5. Positive-ion FAB mass spectrum: *m*/*z* 2158.9 (M^+ − ClO_4, expected isotopic profile), 2057.8 ([M − 2ClO_4]$^+$) and 1029.1 ([M − Cu − 2ClO_4]$^+$). Fourier-transform IR (KBr pellet): $\tilde{\nu}$/cm^{-1} 3063w, 2050s (ν_{CO}), 1987s (ν_{CO}), 1597m, 1567m, 1453s, 1089vs [ν(ClO_4)], 773s, 304 [ν(Ru–Cl)] and 280 [ν(Ru–Cl)] (Found: C, 53.07; H, 3.52; N, 4.78. Calc. for $C_{100}H_{84}Cl_6Cu_2N_8O_{12}P_4Ru_2$: C, 53.25; H, 3.75; N, 4.97%).

Complex 5. A solution of [{$RhCl(C_2H_4)_2$}$_2$] (0.045 g, 0.115 mmol) in CH_2Cl_2 (5 cm^3) was added at room temperature, under argon, to a stirred solution of compound L (0.085 g, 0.230 mmol) in anhydrous CH_2Cl_2 (5 cm^3). During addition the solution turned red-green, then olive-green. After a few minutes the flask was kept under partial vacuum and a white precipitate began to form. After *ca*. 15 min the deep green coloration disappeared and the white precipitate was collected by centrifugation and dissolved in CH_2Cl_2 (*ca*. 150 cm^3). After filtration

hexane in excess was added to the resulting pale yellow solution resulting in the crystallisation of complex **5**. After 2 d at 4 °C the precipitate was collected and dried under vacuum affording the analytically pure white complex **5** (0.122 g, 90%); $R_f = 0.57$ on silica using CH_2Cl_2–MeOH (9 : 1 v/v). ^{1}H NMR ($CDCl_3$): δ 9.83 (m, 1 H), 8.35 (8-line m, 3 H), 8.10 (10-line m, 4 H), 7.91 [d, ^3J(HH) = 7.7 Hz, 1 H], 7.78 (12-line m, 5 H), 7.41 (m, 3 H), 4.06 (4-line m, 1 H, $RhCH_2Cl$), 3.70 (8-line m, 1 H), 3.55–3.40 (m, 2 H) and 3.00–2.82 (m, 2 H). ^{31}P-{^{1}H} NMR ($CDCl_3$): δ +28.3 [d, J(PRh) = 123 Hz]. Fourier-transform IR (KBr pellet): $\tilde{\nu}/cm^{-1}$ 2924m, 1603s, 1444s, 1401s, 1161s, 1101s and 777s. Positive-ion FAB mass spectrum: *m/z* 555.0 ([M − Cl]$^+$, expected isotopic profile), 506.0 ([M − Cl − CH_2-Cl]$^+$) and 471.1 ([M − 2Cl − CH_2Cl]$^+$) (Found: C, 45.87; H, 3.53; N, 3.98. Calc. for $C_{25}H_{23}Cl_3N_2PRh{\cdot}CH_2Cl_2$: C, 46.15; H, 3.72; N, 4.14%).

Complex 6. To a suspension of complex **5** (0.075 g, 0.128 mmol) in CH_2Cl_2–ethanol (1 : 1, 20 cm^3) was added AgO_3SCF_3 (0.035 g, 0.130 mmol) as a solid under argon. After one night of heating at 60 °C, the starting complex was no longer present according to TLC. After filtration of the insoluble silver chloride, the solution was evaporated to dryness and the residue purified by flash chromatography using a 0 to 2% gradient of methanol in CH_2Cl_2; $R_f = 0.27$ on silica using CH_2Cl_2–MeOH (9 : 1 v/v). Recrystallisation from a CH_2Cl_2–hexane mixture afforded the analytically pure complex **6** as yellow crystals (0.048 g, 63%). ^{1}H NMR ($CDCl_3$): δ 9.38 (m, 1 H), 8.14 (3-line m, 4 H), 8.05–7.92 (8-line m, 4 H), 7.84 (3-line m, 3 H), 7.36 (m, 5 H), 4.36 (m, 1 H, $RhCH_2$-OEt), 4.22 (m, 1 H, $RhCH_2OEt$), 3.11 [8-line m, 2 H, (bipy)-$CH_2CH_2PPh_2$], 2.44 [m, 4 H, (bipy)$CH_2CH_2PPh_2$ + OCH_2CH_3] and 0.33 [t, 3 H, ^3J(HH) = 7 Hz, OCH_2CH_3]. ^{13}C-{^{1}H} NMR ($CDCl_3$): δ 131.7, 158.3, 155.3, 148.1, 139.1–121.7 (aromatic C), 72.0 [d, J(CRh) = 17, $RhCH_2O$], 67.4 (s, OCH_2CH_3), 32.10 [d, J(CP) = 54], 19.50 [d, ^2J(CP) = 31 Hz] and 14.5 (s, OCH_2CH_3). ^{31}P-{^{1}H} NMR ($CDCl_3$): δ 27.7 [d, J(PRh) = 132 Hz]. Fourier-transform IR (KBr pellet): $\tilde{\nu}/cm^{-1}$ 2977s, 1646m, 1453m, 1384m, 1262m, 1089m, 1048s and 880m. Positive-ion FAB mass spectrum: *m/z* 565.1 ([M − Cl]$^+$, expected isotopic profile), 506.1 ([M − Cl − $CH_2OCH_2CH_3$]$^+$) and 471.1 ([M − 2Cl − CH_2OEt]$^+$) (Found: C, 51.21; H, 4.41; N, 4.21. Calc. for $C_{27}H_{28}Cl_2N_2OPRh{\cdot}0.5CH_2Cl_2$: C, 51.31; H, 4.54; N, 4.35%).

Acknowledgements

We are grateful to Dr. D. Soulivong and Ms. M. Hissler for the measurement of some NMR and IR spectra.

References

1 See, for example, M. Grassi, G. DeMunno, F. Nicolo and S. Lo Schiavo, *J. Chem. Soc.*, *Dalton Trans.*, 1992, 2367; G. Newkome, *Chem. Rev.*, 1993, **93**, 2067; K. Tani, M. Yabuta, S. Nakamura and T. Yamagata, *J. Chem. Soc.*, *Dalton Trans.*, 1993, 2781; P. Espinet, P. Gómez-Elipe and F. Villafañe, *J. Organomet. Chem.*, 1993, **450**, 145; J. M. Brown, D. I. Hulmes and T. P. Layzell, *J. Chem. Soc.*, *Chem. Commun.*, 1993, 1673; S. D. Perera and B. L. Shaw, *J. Chem. Soc.*, *Chem. Commun.*, 1994, 1201; R.-H. Uang, C.-K. Chan, S.-M. Peng and C.-M. Che, *J. Chem. Soc.*, *Chem. Commun.*, 1994, 2561; R. J. Haines, R. E. Wittrig and C. P. Kubiak, *Inorg. Chem.*, 1994, **33**, 4723; A. Del Zotto, A. Mezzetti and P. Rigo, *J. Chem. Soc.*, *Dalton Trans.*, 1994, 2257; M. Alvarez, N. Lugan and R. Matthieu, *J. Chem. Soc.*, *Dalton Trans.*, 1994, 2755; S. Stoccoro, G. Chelucci, A. Zucca, M. A. Cinulli, G. Minghetti and M. Manassero, *J. Chem. Soc.*, *Dalton Trans.*, 1996, 1295; Z.-Z. Zhang and H. Cheng, *Coord. Chem. Rev.*, 1996, **147**, 1.
2 M. P. Anderson, A. L. Casalnuovo, B. J. Johnson, B. M. Mattson, A. M. Mueting and L. H. Pignolet, *Inorg. Chem.*, 1988, **27**, 1649; A. J. Deeming and M. B. Smith, *J. Chem. Soc.*, *Dalton Trans.*, 1993, 2041; L. Costella, A. Del Zotto, A. Mezzetti, E. Zangrando and P. Rigo, *J. Chem. Soc.*, *Dalton Trans.*, 1993, 3001.
3 A. A. Bahsoun and R. Ziessel, *Nouv. J. Chim.*, 1985, **9**, 225; R. Ziessel, *Tetrahedron Lett.*, 1989, **30**, 463.
4 R. Ziessel, D. Matt and L. Toupet, *J. Chem. Soc.*, *Chem. Commun.*, 1995, 2033.
5 Th. Kauffmann, J. König and A. Waltermann, *Chem. Ber.*, 1976, **109**, 3864.
6 R. Colton and R. H. Farthing, *Aust. J. Chem.*, 1967, **20**, 1283.
7 MolView, J. M. Cense, Ecole Nationale Superieure de Chimie de Paris, 1990.
8 E. M. Hyde, J. D. Kennedy and B. L. Shaw, *J. Chem. Soc.*, *Dalton Trans.*, 1977, 1571.
9 M. J. Cleare and W. P. Griffith, *J. Chem. Soc. A*, 1969, 372; C. F. J. Barnard, J. A. Daniels, J. Jeffery and R. J. Mawby, *J. Chem. Soc.*, *Dalton Trans.*, 1976, 953.
10 M.-N. Collomb-Dunand-Sauthier, A. Deronzier and R. Ziessel, *J. Chem. Soc.*, *Chem. Commun.*, 1994, 189.
11 M.-N. Collomb-Dunand-Sauthier, A. Deronzier and R. Ziessel, *Inorg. Chem.*, 1994, **33**, 2961.
12 S. Chardon-Noblat, A. Deronzier, D. Zsoldos, R. Ziessel, M. Haukka, T. A. Pakkanen and T. Venäläinen, *J. Chem. Soc.*, *Dalton Trans.*, 1996, 2581.
13 S. Chardon-Noblat, M.-N. Collomb-Dunand-Sauthier, A. Deronzier, R. Ziessel and D. Zsoldos, *Inorg. Chem.*, 1994, **33**, 4410.
14 M.-N. Collomb-Dunand-Sauthier, A. Deronzier and R. Ziessel, *J. Electroanal. Chem.*, *Interfacial Electrochem.*, 1993, **350**, 43.
15 B. J. Hathaway, D. G. Holah and J. D. Poslethwaite, *J. Chem. Soc.*, 1961, 3215.
16 A. Bilyk and M. M. Harding, *J. Chem. Soc.*, *Dalton Trans.*, 1994, 77; A. Bilyk, M. M. Harding, P. Turner and T. W. Hambley, *J. Chem. Soc.*, *Dalton Trans.*, 1994, 2783.
17 D. Zurita, C. Scheer, J.-L. Pierre and E. Saint-Aman, *J. Chem. Soc.*, *Dalton Trans.*, 1996, 4331.
18 See, for example, Y. C. Lin, J. C. Calabrese and S. S. Wreford, *J. Organomet. Chem.*, 1983, **105**, 1679; H. Werner, L. Hofmann, R. Feser and W. Paul, *J. Organomet. Chem.*, 1985, **281**, 317; B. Weinberger, G. Tanguy and H. DesAbbayes, *J. Organomet. Chem.*, 1985, **280**, C31; T. B. Marder, W. C. Fultz, J. C. Calabrese, R. L. Harlow and D. Milstein, *J. Chem. Soc.*, *Chem. Commun.*, 1987, 1543.
19 J. Suffert, *J. Org. Chem.*, 1989, **54**, 509.
20 N. G. Walker and D. Stuart, DIFABS, *Acta Crystallogr.*, *Sect. A*, 1983, **39**, 158.
21 *International Tables for X-Ray Crystallography*, D. Riedel, Boston, MA, 1983, p. 183.
22 C. K. Fair, MOLEN, An Interactive Intelligent System for Crystal Structure Analysis, Enraf-Nonius, Delft, 1990.

Received 10*th April* 1997; *Paper* 7/02463K